

# A Conceptual Model for Effective Directional Emissivity from Nonisothermal Surfaces

Xiaowen Li, Alan H. Strahler, *Member, IEEE*, and Mark A. Friedl

**Abstract**—The conventional definition of emissivity requires the source of radiation to be isothermal in order to compare its thermal emission to that of a blackbody at the same temperature. This requirement is not met for most land surfaces considered in thermal infrared remote sensing. Thus, the effective or equivalent emissivity of nonisothermal surfaces has been a poorly defined but widely used concept for years. Recently, several authors have attempted to define this concept more clearly. Unfortunately, definitions such as ensemble emissivity (e-emissivity) and emissivity derived from the surface bidirectional reflectance distribution function (r-emissivity) [27] do not fully satisfy current needs for estimating true land surface temperature (LST). We suggest the use of an additional term, the “apparent emissivity increment,” which considers the effects of geometric optics to explain the directional and spectral dependence in LST caused by the three-dimensional (3-D) structure and subpixel temperature distribution of the surface. We define this quantity based upon the emissivity derived from the bidirectional reflectance distribution function ( $\epsilon_{\text{BRDF}}$ ) for isothermal surfaces and present a conceptual model of thermal emission from nonisothermal land surfaces. Our study also indicates that an average LST corresponding to the hemispherical wideband  $\epsilon_{\text{BRDF}}$  will be useful in remote sensing-based LST modeling and inversion.

**Index Terms**—BRDF, brightness temperature, emissivity, geometric optics, land surface temperature.

## I. INTRODUCTION

TEMPERATURE and emissivity are two fundamental physical properties that are defined simply and easily for homogeneous, isothermal surfaces. However, natural land surfaces are neither homogeneous nor isothermal. Moreover, they emit thermal radiance anisotropically. Thus, a need exists for formal definitions of “effective” surface temperature and “effective” emissivity that can be applied to such surfaces and that also can serve as a basis for temperature and emissivity retrievals from remote sensing.

Land surface temperature (LST) measurements derived from aircraft and spaceborne sensors include information related to both land surface properties, land surface radiation and energy balance, and interactions between the land surface and atmospheric planetary boundary layer [32], and therefore are quite complex. Accurate methods to retrieve LST from

remote sensing are required for a wide variety of geophysical research domains, including estimation of soil moisture using thermal inertia techniques [6], [29], geothermal mapping [17], [18], [41], and inversion of sensible and latent heat fluxes from land surfaces using energy balance models [7], [9], [10], [13], [21], [34], [37], [42]. In more applied domains such as agriculture, canopy temperatures have been used to evaluate water requirements of wheat [16], to determine frosts in orange groves [8], and to map frost-damaged areas [19].

For many of these problem domains, however, the uncertainty associated with remotely sensed estimates of LST has severely limited the utility of such data. In particular, uncertainty in LST measurements may be attributed to three main sources. First, atmospheric absorption and emission of thermal radiation can introduce substantial bias to estimates of LST from aircraft- and satellite-measured thermal radiances. Second, uncertainty regarding the emissivity of surface materials can introduce error to estimates of LST converted from brightness temperatures. Third, land surface heterogeneity and three-dimensional (3-D) structure can produce significant variation in LST measurements as a function of view zenith angle. In recent years, a number of temperature retrieval algorithms have been developed to overcome the first two sources of uncertainty identified previously. These algorithms include temperature emissivity separation (TES) [14], [33], modified split-window methods [2], [3], [28], [30], [31], [38], [39], the day/night method [25], [40], and the multipixel method [26], [36].

Problems associated with directional dependence in LST measurements, on the other hand, have proven to be both substantial and difficult to solve. Kimes *et al.* [20], for example, showed that the effective radiant temperature of a three-layer canopy may exhibit differences of 2 K as view zenith angles vary from near horizontal to near nadir. Similarly, Dozier and Warren [12] showed that the directional emissivity of snow surfaces may produce as much as 3 K angular variation in brightness temperature. More importantly, directional effects associated with land surface structural properties at larger scales can produce even higher angular variation in measured LST. For example, Balick and Hutchinson [1] reported a 7 K angular variation in effective radiant temperature over a leafless deciduous forest. These levels of uncertainty significantly reduce the utility of LST measurements for many geophysical applications. Thus, there is a pressing need to account for directional viewing effects in LST measurements.

The objective of this paper is to present a new conceptual model that accounts for the effects of 3-D structure

Manuscript received August 5, 1998; revised December 28, 1998. This work was supported in part by China's National Key-Important Basic Research Plan and in part by NASA Grants NAS 5-31369 and NAG 5-7217, and in part by NSF Grant EAR-9725698.

X. Li is with the Research Center for Remote Sensing and GIS, Beijing Normal University, Beijing 100875, China.

A. H. Strahler and M. A. Friedl are with the Department of Geography and Center for Remote Sensing, Boston University, Boston, MA 02215 USA.

Publisher Item Identifier S 0196-2892(99)06280-4.

and subpixel heterogeneity on directional variation in LST measurements. To accomplish this goal, the model presents a method to compute the effective emissivity of a nonisothermal surface. That is, it presents a method to compute the equivalent emissivity that would produce the observed LST for an isothermal surface. This concept has been used rather widely since the 1970's, but only recently has it been defined in a formal sense [4], [27], [38]. However, as we shall demonstrate later in the text, these definitions still do not meet the needs of LST remote sensing of nonisothermal surfaces.

The conceptual model described in this paper builds upon previous work in this domain by integrating the effects of both geometric optics and multiple scattering imposed by 3-D structure in nonisothermal surfaces. To present this model, the paper is structured as follows. We first discuss the basic physics of radiation emission that underlay all LST measurements. This section is followed by an explanation of the key factors that require consideration when nonisothermal surfaces are of interest, in association with a simple example to illustrate our points. We then present a formal definition of our conceptual model along with a simple strategy for its inversion. We conclude with a summary of the key points of our model and a brief discussion of its limitations.

## II. BASIC LAWS AND TERMINOLOGY

### A. Planck Law and Emissivity

All objects with temperatures greater than 0 K emit radiation. Emission from a blackbody surface follows the Planck radiation law

$$B_{\lambda}(T) = \frac{C_{\lambda}}{\exp(D_{\lambda}/T) - 1} \quad (1)$$

where  $\lambda$  is the wavelength  $C_{\lambda}$  and  $D_{\lambda}$  are known functions of  $\lambda$  but are invariant with respect to temperature  $T$ . That is

$$C_{\lambda} = \frac{1.191 \times 10^8}{\lambda^5}$$

$$D_{\lambda} = \frac{1.439 \times 10^4}{\lambda}$$

where  $\lambda$  is a wavelength in  $\mu\text{m}$ , providing  $B_{\lambda}(T)$  in units of  $\text{Wm}^{-2} \text{sr}^{-1} \mu\text{m}^{-1}$ .

The magnitude and spectral distribution of energy emitted from a uniform surface is a function of its thermodynamic temperature and "spectral emissivity." Spectral emissivity is defined as the ratio of the spectral exitance emitted by a surface to the spectral exitance emitted by a blackbody at the same temperature. Therefore, spectral emissivity is defined strictly only for isothermal surfaces. In this paper, we only consider spectral, or more accurately band-averaged, emissivity or radiance. Therefore, the term spectral and the corresponding subscript  $\lambda$  will not be used unless specifically needed. "Directional emissivity"  $\varepsilon(\mu)$ , where  $\mu$  is the direction of emission or viewing, is defined similarly. Note that an ideal blackbody surface emits isotropically. In other words, the radiance emitted in direction  $\mu$  from a surface at thermodynamic temperature  $T$  is given by the product of its

directional emissivity and the Planck function

$$L(\mu) = \varepsilon(\mu) \times B(T). \quad (2)$$

"Directional brightness temperature" can be found by solving the Planck function for  $T$ , using the observed directional emitted radiance  $L(\mu)$ , as if  $L(\mu)$  were emitted from a blackbody. Note that directional brightness temperature is wavelength dependent if  $\varepsilon(\mu)$  varies with wavelength.

A variety of terminology has been used to describe LST. For example, when environmental downwelling thermal radiance is of concern, terms such as "effective radiant temperature" and "effective brightness temperature" have been used (e.g., [1], [20]). A related variable that is very difficult to measure from remote sensing is the surface "aerodynamic temperature," which is the temperature of the surface at the effective level of sensible heat exchange. In this paper, we consider exclusively the surface skin temperature, which controls the instantaneous directional thermal emission from land surfaces. We therefore consider only instantaneous quantities and assume no downwelling environmental thermal radiance. This assumption is employed to simplify the problem examined in this paper. However, it will introduce small levels of error to estimates of LST and therefore will need to be considered in future versions of the model presented below.

Note that in both (1) and (2), the temperature  $T$  is independent of wavelength and direction. Since  $B(T)$  is a universally applicable and known function, and emissivity is determined by material characteristics and can be measured in the laboratory, (2) is very convenient for practical application. However, (1) and (2) require the surface to be isothermal. Here, the term "isothermal surface" is not used in a strict sense. Rather, we define isothermal to mean that there are no notable spatial patterns of distinct temperature differences over the surface of interest. That is, if the surface temperature has a continuous probability density distribution within a small range, and the spatial distribution of surface elements at different temperatures is random, then (1) and (2) still apply to the average temperature of the surface. This is true because the Planck Law itself is based on statistical physics. Conversely, if distinct and systematic temperature differences are present (for example when canopy leaves have a temperature distinct from the underlying soil) then (1) and (2) do not apply, and we will refer to such a surface as nonisothermal.

### B. Kirchhoff's Law and Emissivity for Nonisothermal Surfaces

Kirchhoff's law relates the spectral reflectance of a surface to its spectral emissivity

$$\varepsilon = 1 - r \quad (3)$$

where  $\varepsilon$  and  $r$  are hemispherical properties. It also can be written as

$$\varepsilon(\mu) = 1 - r(\mu) \quad (4)$$

where  $r(\mu)$  is the directional-to-hemispherical reflectance. Note that the temperature of the surface does not enter into (3) and (4). However, Kirchhoff's Law was derived under the assumption of thermal equilibrium, and therefore, an

isothermal surface is implied. Dozier and Warren [12] used this law to define and to calculate the directional emissivity of snow from the hemispherical integration of its bidirectional reflectance distribution function (BRDF).

Because (1)–(4) do not apply to nonisothermal surfaces, a variety of work has been attempted recently to define the emissivity of such surfaces [4], [27], [39]. An intuitive way to do this is to treat the surface as a blackbody ensemble with exactly the same structure and temperature distribution as the real surface. The emissivity is then the ratio of the emission from the surface to the blackbody ensemble. Norman and Becker [27] refer to this quantity as the ensemble emissivity (e-emissivity for short). However, there are several problems with this definition. First, it is almost impossible to construct a blackbody surface with the same structure and temperature distribution as the real surface. Thus, e-emissivity cannot be measured in practice. Second, e-emissivity precludes formal definition of a function describing the emission from such a blackbody ensemble. That is, there is no average temperature that will yield the correct emission using the Planck Law if the ensemble has two distinctive peaks in its surface temperature distribution. Therefore, the practical and theoretical merits of this definition are limited.

A more promising definition, also proposed by Norman and Becker [27], follows that of Dozier and Warren [12]. This definition uses (4) to define a directional emissivity for nonisothermal surfaces and refers to it as the directional r-emissivity. This definition has the advantage that the surface emissivity is determined by the material emissivities and structure of the surface and is independent of the subpixel distribution of temperature values. Therefore, r-emissivity can be treated as an intrinsic property of the surface in question. Unfortunately, however, r-emissivity is wavelength and view geometry specific, and therefore is not useful for explaining or predicting the spectral and directional dependence of emission from nonisothermal surfaces.

As a simple example, assume that a flat surface consists of one area ( $a_1$ ) with temperature  $T_1$ , with the remaining area  $a_2 = 1 - a_1$  possessing temperature  $T_2$  [Fig. 1(a)]. The thermal directional emission from this surface is

$$L_\lambda(T_0) = \epsilon_r [a_1 B_\lambda(T_1) + a_2 B_\lambda(T_2)]$$

where  $\epsilon_r$  is the r-emissivity, and  $T_0$  is the effective brightness temperature determined by  $L_\lambda$ . If we further assume that the surface behaves as a blackbody so that  $\epsilon_r = 1.0$ ,  $T_0$  is then

$$T_0 = B_\lambda^{-1} [a_1 B_\lambda(T_1) + a_2 B_\lambda(T_2)] \\ = \frac{D_\lambda}{\ln \left( \frac{C_\lambda}{a_1 B_\lambda(T_1) + a_2 B_\lambda(T_2)} + 1 \right)}$$

However, because the Planck equation is nonlinear with respect to wavelength,  $T_0$  is wavelength dependent unless  $T_1 = T_2$ . Further, if the surface isn't flat [Fig. 1(b)] and thus  $a_1$  and  $a_2$  vary with view direction,  $T_0$  also will be direction dependent. Therefore, a general function for  $B_\lambda(T(\lambda, \mu))$  cannot be defined based upon r-emissivity. Also, note that in this case, we may intuitively define  $T_0 = a_1 T_1 + a_2 T_2$ . This

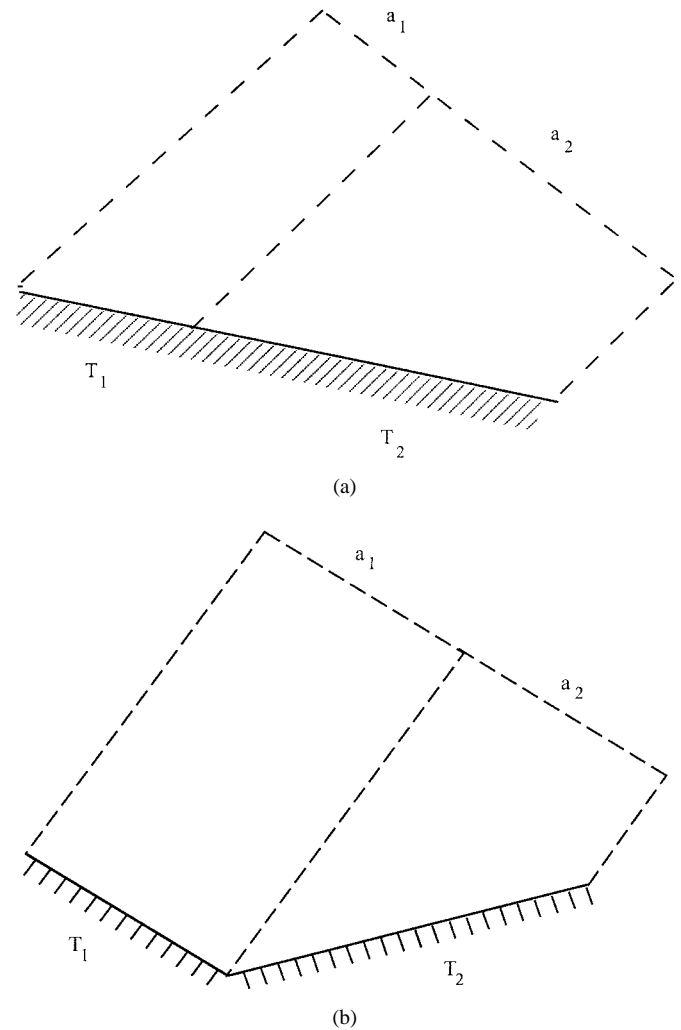


Fig. 1. Schematics showing (a) flat nonisothermal surface and (b) nonisothermal surface with variation in elevation at subpixel scales.

linearization will probably be correct in many applications, but it will yield a wavelength-dependent effective emissivity that is greater than 1.0 at some wavelengths and less than a 1.0 at other wavelengths.

Finally, Wan and Dozier [38] define the average emissivity as the area-weighted sum of material emissivities. This is actually a special case of r-emissivity, and thus includes the same advantages and drawbacks identified above. For the sake of clarity, we will call this directional r-emissivity the BRDF-derived emissivity ( $\epsilon_{\text{BRDF}}$  for short).

### C. Models for Directional Thermal Emission

The model presented by Dozier and Warren [12] describes the directional thermal emission from an (isothermal) snow surface. The model is BRDF-driven, using (4) directly, and in theory it can be used for other isothermal surfaces as well. We will refer to this as the DW BRDF model. A special advantage of the DW BRDF model is that multiple scattering of thermal emission within the surface structure can be taken into account through BRDF modeling.

For nonisothermal surfaces, the Kimes–Smith–Link model may be used to compute directional emission [20]. This model

employs a pure geometric-optical (GO) approach to interpret directional thermal emission. It is simple and straightforward and explained the directional variation in canopy emission very well for the cases they considered in which temperature differences from the canopy top to bottom were as large as 4 K. We will refer to this model as the KSL GO model.

The KSL GO model is in essence a gap probability model in which the total surface emission is computed as the area-weighted sum of emissions from different depths within the canopy visible in the sensor's field of view (FOV). Multiple scattering is ignored in the KSL GO model, which may be very important in the thermal wavelength region even when single scattering is very weak. For example, if we assume a homogeneous, isothermal, and semi-infinite canopy layer, the KSL GO model will yield a canopy temperature/emissivity pair identical to that of a single leaf, since the sensor's FOV is full of the leaves with the same temperature and emissivity in this case. Further, the emission from the canopy will be isotropic. However, LST measurements over optically thick canopies tend to show emissivities that are higher than the individual leaves within the canopy, and also exhibit notable directional dependence. As we will demonstrate later in the text, these properties are explained by multiple scattering.

To summarize, the DW BRDF model works well for isothermal surfaces, but is not suitable for nonisothermal surfaces. The KSL GO model, on the other hand, works well for surfaces in which temperature differences are large but fails when temperature differences are small and multiple scattering is not negligible. Therefore, we require a new model that is suitable for nonisothermal surfaces and that converges to the DW BRDF model when the temperature differences within the sensor FOV become small. As a solution, we present a new model that uses the KSL GO model to calculate  $L(T)$  and the corresponding effective emissivity ( $\varepsilon_{\text{GO}}(T|T_0)$ ) from inversion of the Planck function, given a reference temperature  $T_0$ .

### III. SIMPLE ILLUSTRATIVE CASE: FLAT SURFACE MIXTURE

To illustrate these concepts, we begin by assuming that a flat surface consists of two components possessing areas  $a_1$  and  $a_2$  in direction  $\mu$ , emissivities  $\varepsilon_1$  and  $\varepsilon_2$ , and true component temperatures  $T_1$  and  $T_2$ , respectively [Fig. 1(a)]. For simplicity, the surface is assumed to be gray (i.e., both  $\varepsilon_1$  and  $\varepsilon_2$  are independent of wavelength and viewing direction). The total emission from this surface in direction  $\mu$  is then computed as

$$L_\lambda(T_0) = a_1\varepsilon_1 B_\lambda(T_1) + a_2\varepsilon_2 B_\lambda(T_2) \quad (5)$$

where  $T_0$  is the brightness temperature estimated by inversion of the Planck equation, independent of wavelength and viewing direction.

To obtain an effective emissivity  $\varepsilon_0$  for this surface, we rewrite (5) as

$$L_\lambda(T_0) = \varepsilon_0(\lambda) B_\lambda(T_0). \quad (6)$$

Note that  $\varepsilon_0$  is a function of wavelength because a single value for  $T_0$  cannot be used to predict  $B(T_0)$  as a linear

combination of  $B_\lambda(T_1)$  and  $B_\lambda(T_2)$  for all wavelengths if  $T_1 \neq T_2$ . In other words, nonisothermal gray (or blackbody) surfaces do not behave as gray (or black) surfaces. To handle this problem, the theories behind both r- and e-emissivities attempt to preserve graybody emissivity at the expense of using an ensemble blackbody or introducing new variables into the Planck function such as a wavelength and direction dependent  $T_0$ .

Here, we propose a different definition that requires  $T_0$  be independent of wavelength and direction and also be constant everywhere within the surface of interest. To do this, we assume  $T_1 < T_2$ , and define

$$\begin{aligned} \Delta T_1 &= T_0 - T_1 \\ \Delta T_2 &= T_2 - T_0. \end{aligned}$$

Using a first-order Taylor series approximation, we have

$$B_\lambda(T_2) = B_\lambda(T_0) + B'_\lambda(T_0)\Delta T_2 \quad (7)$$

$$B_\lambda(T_1) = B_\lambda(T_0) - B'_\lambda(T_0)\Delta T_1 \quad (8)$$

where  $B'_\lambda(T_0)$  is the first derivative of  $B_\lambda$  at temperature  $T_0$ . This can be expressed as  $B_\lambda(T_0) \times K_\lambda(T_0)$ , where  $K_\lambda(T_0)$  has dimensions of inverse temperature and is a known function of  $\lambda$  and  $T$

$$K_\lambda(T_0) = \frac{D_\lambda e^{D_\lambda/T_0}}{T_0^2 (e^{D_\lambda/T_0} - 1)}.$$

Then, by combining (5) and (6), we have

$$\varepsilon_0(\lambda) = [a_1\varepsilon_1 + a_2\varepsilon_2] + [(a_2\varepsilon_2\Delta T_2 - a_1\varepsilon_1\Delta T_1)K_\lambda(T_0)]. \quad (9)$$

Therefore, if we define  $T_0$  such that

$$a_2\varepsilon_2\Delta T_2 = a_1\varepsilon_1\Delta T_1$$

or

$$T_0 = [a_2\varepsilon_2 T_2 + a_1\varepsilon_1 T_1] / [a_2\varepsilon_2 + a_1\varepsilon_1]$$

then to a first-order approximation, we obtain a wavelength independent effective emissivity

$$\varepsilon_0 = a_1\varepsilon_1 + a_2\varepsilon_2.$$

Unfortunately, this cannot be extended to more complicated cases in which  $a_1$  and  $a_2$  change with viewing direction, or when  $\varepsilon_1$ ,  $\varepsilon_2$  are not both gray. We shall address this problem later and refer to  $T_0$  as the "reference temperature," which is the temperature of a blackbody used to quantify the effective emissivity of the nonisothermal surface.

More importantly, note that the right hand side of (9) is composed of two distinct parts. The first part  $a_1\varepsilon_1 + a_2\varepsilon_2$  is simply the  $\varepsilon_{\text{BRDF}}$  of the pixel, independent of the reference temperature  $T_0$ , while the second part reflects the influence of the geometric optics. That is

$$\begin{aligned} &(a_2\varepsilon_2\Delta T_2 - a_1\varepsilon_1\Delta T_1)K_\lambda(T_0) \\ &= \varepsilon_{\text{GO}}(T|T_0) - \varepsilon_{\text{GO}}(T_0|T_0) = \Delta\varepsilon_{\text{GO}}(T|T_0). \end{aligned}$$

Therefore, we can rewrite (9) as

$$\varepsilon_0(\lambda) = \varepsilon_{\text{BRDF}} + \Delta\varepsilon_{\text{GO}}(T|T_0). \quad (10)$$

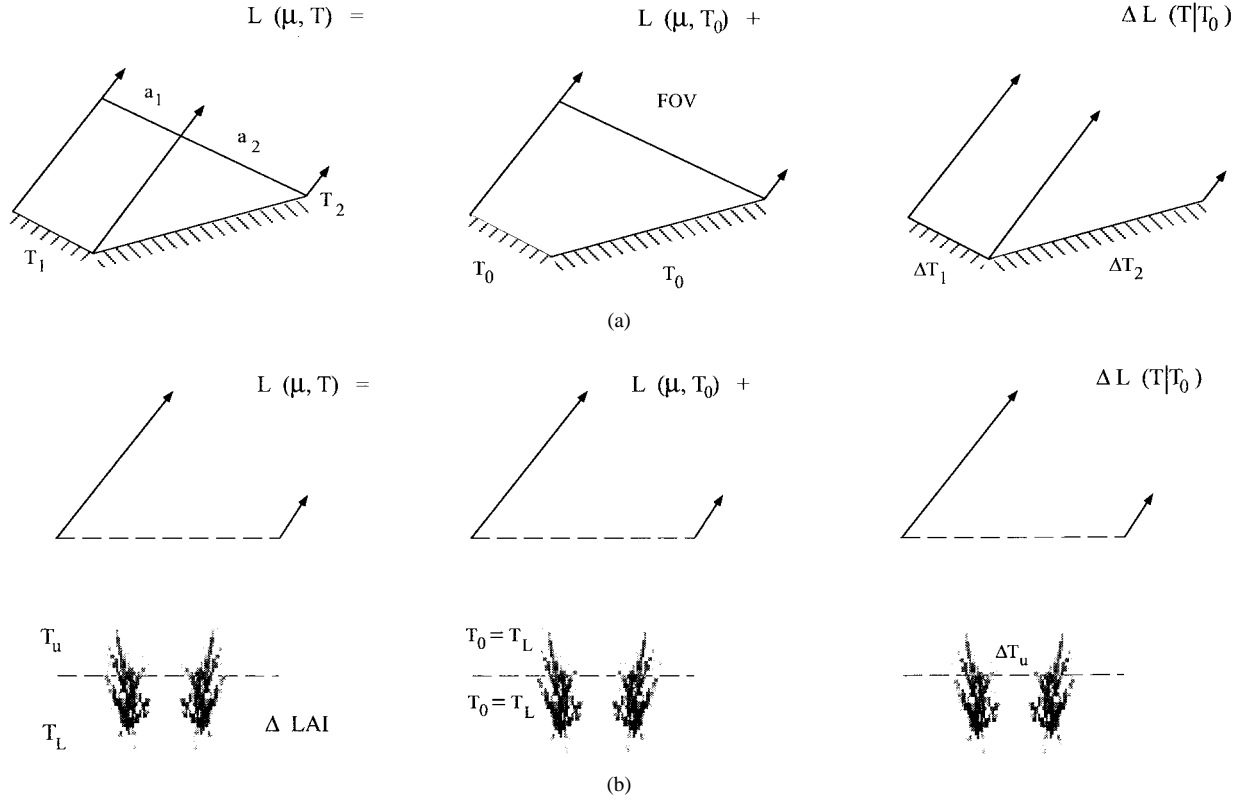


Fig. 2. Schematics illustrating the conceptual basis for the model. The radiance leaving nonisothermal surfaces ( $L(T, \mu)$ ) is decomposed into two components: the equivalent radiance from an isothermal surface at temperature  $T_0$  ( $L(T_0, \mu)$ ) and the change in radiance due to the subpixel temperature distribution  $\Delta L(T|T_0)$  for: (a) unvegetated and (b) vegetated surfaces.

Here,  $\varepsilon_{GO}$  is the KSL GO emissivity, and  $\Delta\varepsilon_{GO}(T|T_0)$  is the change in  $\varepsilon_{GO}$  induced by the nonisothermal temperature distribution ( $T|T_0$ ), given reference temperature  $T_0$ . In other words, given a reference temperature  $T_0$ , the effective emissivity of a flat, nonisothermal surface consists of two parts: the BRDF-derived emissivity and the apparent emissivity increment caused by the nonisothermal nature of the surface.

It is most accurate to call the product  $\Delta\varepsilon_{GO}(T|T_0)B_\lambda(T_0)$  the “apparent increment in thermal emittance,” and the term  $a_2\varepsilon_2\Delta T_2 - a_1\varepsilon_1\Delta T_1$  the “increment of apparent temperature due to a nonisothermal temperature distribution.” However, since  $\Delta\varepsilon_{GO}$  has units of emissivity (dimensionless), it is preferable to have a single term or concept to describe our result obtained using a conventional blackbody of temperature  $T_0$ . We refer to this quantity as the transformed emissivity increment from the “apparent increment in thermal emittance.” Despite this rather cumbersome terminology, the additional term  $\Delta\varepsilon_{GO}(T|T_0)$  provides us with the best approach to dealing with the dual problems of both directional and spectral dependence of emission from nonisothermal surfaces, while keeping the Planck function (as well as the conventional blackbody) and BRDF-derived emissivity unchanged.

#### IV. EFFECTIVE EMISSIVITY OF A NONISOTHERMAL SURFACE

We now consider the more general case in which the surface possesses 3-D structure. Here, the area proportions of two distinct components within the field of view may change with

view direction [Fig. 1(b)]. Intuitively, we may write

$$L_\lambda(\mu, T_0) = a_1(\mu)\varepsilon_1B_\lambda(T_1) + a_2(\mu)\varepsilon_2B_\lambda(T_2). \quad (11)$$

However, because the two components no longer lie together on a flat surface, multiple scattering between them now must be taken into account.

We begin by assuming that the emission from every surface facet can be approximated by the first two terms of a Taylor series. Using the example from the previous section, we consider the surface to be composed of two isothermal facets possessing different temperatures. The thermal emission from the surface may then be approximated as a function of  $T_0$  where the effective emissivity of the surface includes the effects of both multiple scattering (through  $\varepsilon_{BRDF}$ ) and geometric optics [through  $\Delta\varepsilon_{GO}$ , Fig. 2(a)]. This approach therefore includes elements of both the DW BRDF model and the KSL GO model

$$L_\lambda(\mu, T_0) = [\varepsilon_{BRDF} + \Delta\varepsilon_{GO}(T|T_0)]B_\lambda(T_0) \quad (12)$$

or

$$\varepsilon_0(\mu, \lambda) = \varepsilon_{BRDF} + \Delta\varepsilon_{GO}(T|T_0) \quad (13)$$

where

$$\Delta\varepsilon_{GO}(T|T_0) = (a_2(\mu)\varepsilon_2\Delta T_2 - a_1(\mu)\varepsilon_1\Delta T_1)K_\lambda(T_0). \quad (14)$$

Although (13) has the same form as (10), note that  $\varepsilon_{BRDF}$  in (13) now includes multiple scattering and  $\Delta\varepsilon_{GO}$  includes directional effects caused by the combined effects of 3-D

structure and temperature differences within the sensor FOV. In addition, unlike a flat, nonisothermal surface, it is now impossible to define a  $T_0$  that causes the  $\Delta\varepsilon$  term to be zero for all viewing directions. Of course,  $T_0$  still can be defined such that the hemispherical emissivity accounts for the  $\Delta\varepsilon$  term, if needed. In such cases, the hemispherical average  $\varepsilon_0$  then becomes the same as the hemispherical r-emissivity as defined by Becker and Li [4]. Note that unlike earlier work,  $T_0$  is defined simultaneously with  $\varepsilon_0$  in our model. Similarly, when  $\varepsilon_1, \varepsilon_2$  are not both gray,  $T_0$  will become wavelength dependent, and a wide-band average (for example, 8–14  $\mu\text{m}$  to cover the peak of the Planck function for usual LST's) can be used to approximate a hemispheric, wide-band-effective emissivity, intrinsic to the surface material and structure.

To illustrate how this conceptual model works, as well as how it relates to the DW BRDF and KSL GO models, we now consider a homogeneous, semi-infinite leaf canopy. We assume that the canopy has isothermal leaves at temperature  $T_0$ , a spherical leaf angle distribution (LAD), leaf facets with Lambertian reflectance  $\rho = 0.04$  (opaque to thermal radiation), and that the emissivity of a single leaf is 0.96. Following Hapke [15], the directional hemispherical reflectance of the semi-infinite canopy layer will then be

$$r(\mu) = (1 - \gamma)/(1 + 2\gamma\mu) + 0.25\rho\mu/(1 + 2\mu)$$

where  $\mu$  is the cosine of incidence angle and  $\gamma = \sqrt{1 - \rho} = 0.98$ . Therefore

$$r(\mu) = 0.02/(1 + 1.96\mu) + 0.01\mu/(1 + 2\mu).$$

When the incidence angle changes from nadir to nearly horizontal,  $r(\mu)$  changes from 0.01 to 0.02. This means that the directional emissivity of the canopy will vary from 0.99 (nadir) to 0.98 (horizontal). This agrees very well with observations and is usually explained by the assumption that gaps within the canopy behave like blackbodies. In other words, because nadir views see deeper into the canopy, they possess a higher effective emissivity. The DW BRDF model with Hapke's formulation therefore provides a quantitative description of these relationships. The KSL GO model fails in this case, because multiple scattering is ignored [20]. It can be argued that the KSL GO model still may work if the brightness temperature at different depths is used instead of the true emitted radiance temperature. However, this calculation is so complicated that the merits of the KSL model may be lost.

We now assume that the top layer of the canopy, possessing a leaf area index ( $\Delta_{\text{LAI}}$ ) of 2.0, is 4° cooler than the layer below [Fig. 2(b)]. For the range of typical temperatures encountered in vegetation canopies, the DW BRDF model predicts between 0.7–1 K directional variation produced by a variation of 0.01 in directional emissivity. The KSL GO model, however, predicts a variation in directional LST from nadir to near horizontal viewing of roughly 1.5 K. Thus, the DW BRDF model is unable to explain the directional variation in canopy emission caused by strong temperature differences within the canopy.

When our conceptual model (13) is applied to these two cases, we see that these limitations are resolved. Specifically,

in the first case (semi-infinite canopy), since  $\Delta\varepsilon$  is zero, (13) is in fact the same as DW BRDF model. In the second case ( $\Delta_{\text{LAI}} = 2.0$ ), in addition to 0.01 directional variation predicted from  $\varepsilon_{\text{BRDF}}, \varepsilon_{\text{GO}}$  provides between 0.02–0.04 variation in directional variability of effective emissivity. The exact values depend on the reference temperature ( $T_0$ ) and wavelength selected. More importantly, for representative ranges of canopy temperatures, (13) captures the effects of both multiple scattering and differences in temperatures within the canopy.

On a related note, there may be concern as to whether or not the first-order Taylor approximation is sufficiently accurate for practical applications. Note that the second order derivative of Planck function has the form

$$B_\lambda(T)K_\lambda^2(T) + B_\lambda(T)K_\lambda'(T).$$

If we use Einstein's approximation for  $K_\lambda(T)$ , the form of the second-order derivative of Planck function is rather simple, since

$$K_\lambda'(T) = -2K_\lambda(T)/T.$$

Thus, our approach to preserve the Planck function is still valid, but one additional correction term is added to account for temperature differences within the sensor FOV. Since high-order derivatives can be obtained in a similar form, in theory this conceptual model can be extended to have very high accuracy for flat, nonisothermal mixtures. For nonisothermal surfaces possessing 3-D structure, the only required assumption is that the multiple scattering between the virtual surfaces possessing temperature differences be ignored.

## V. MODEL EXTENSION AND INVERSION

Clearly, many surfaces are composed of a mixture of more than two isothermal components. For example, forest scenes (e.g., [23]) include sunlit crown, sunlit soil, shaded crown, and shaded soil, and therefore may have up to four distinctive temperatures. In this type of scenario, the model easily can be extended to

$$\Delta\varepsilon_{\text{GO}}(T|T_0) = K_\lambda(T_0) \sum_i a_i(\mu)\varepsilon_i\Delta T_i \quad (15)$$

where  $\Delta T_i = T_i - T_0$ , and  $\sum_i a_i(\mu) = 1.0$ . Inversion of this model is difficult. Below, we present a simple example for illustration.

First, we consider a nonisothermal canopy such as the one described in Section IV, with the temperature of the upper layer of the canopy ( $T_u$ ) = 296 K and the temperature of the lower canopy ( $T_l$ ) = 300 K. The directional and spectral thermal emission from the canopy is approximated using an arbitrary reference temperature  $T_0 = T_l$ . Then, the only temperature increments are in the top layer. Using (12)–(15), this yields

$$\begin{aligned} L_\lambda(\mu, T_0) &= [\varepsilon_{\text{BRDF}} + \Delta\varepsilon_{\text{GO}}(T|T_0)]B_\lambda(T_0) \\ &= [(1 - r(\mu)) - 4.0 \times 0.96 \times (1 - X(\mu)) \\ &\quad \times K_\lambda(T_0)]B_\lambda(T_0) \end{aligned} \quad (16)$$

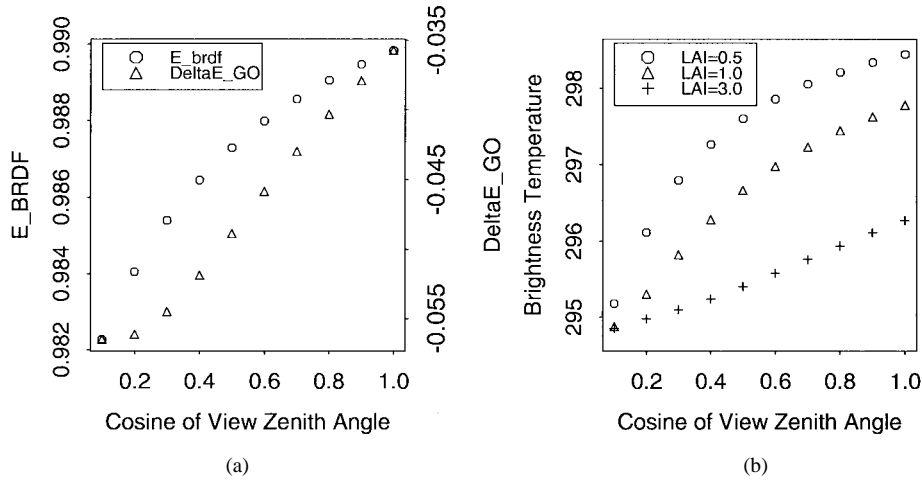


Fig. 3. Simulated values for: (a)  $\epsilon_{\text{BRDF}}$  and  $\Delta\epsilon_{\text{GO}}$  ( $\Delta_{\text{LAI}} = 2.0$ ) and (b) brightness temperature for  $\Delta_{\text{LAI}} = 0.5, 1.0,$  and  $3.0$ .

TABLE I

$\mu$	$D(\mu)$
1.0	0.753569
0.8	0.416568
0.6	0.011826
0.4	-0.432139
0.2	-0.749824

where 4.0 is the temperature difference between  $T_u$  and  $T_0$ , 0.96 is the emissivity of the leaves in the canopy, and for the sake of conciseness,  $X(\mu) = 1 - X(\mu) \exp(-0.5 * \Delta_{\text{LAI}}/\mu)$  is the fraction of the sensor FOV occupied by the upper layer of the canopy. Note that the selection of an arbitrary reference temperature between  $T_u$  and  $T_l$  has little effect on simulated values of  $L_\lambda(\mu, T_0)$  for the given conditions. For example, using  $\lambda = 11 \mu\text{m}$  and varying the cosine of the view zenith from  $\mu = 0.1$  to  $1.0$  in steps of  $0.1$ , the maximum difference between estimates of  $L_\lambda$ , caused by using  $T_0 = 296$  versus  $T_0 = 300$  K as reference temperatures, is less than  $0.16\%$ . Forward mode simulations for brightness temperature  $\epsilon_{\text{BRDF}}$  and  $\epsilon_{\text{GO}}$  using this example are shown in Fig. 3. In the following, the ten simulated values for  $L_\lambda(\mu, T_l)$  are treated as measured values.

We now assume that multiangular measurements of  $L_\lambda(\mu)$  are available, and that the leaf emissivity and LAD (spherical) are known. Our unknowns are then  $T_l$ ,  $T_u$ , and the thickness of the top layer of the canopy ( $\Delta_{\text{LAI}}$ ). The inversion problem therefore requires solution for four unknowns  $T_u$ ,  $T_l$ ,  $T_0$ , and  $\Delta_{\text{LAI}}$  from the equations

$$L_\lambda(\mu, T_0) = [(1 - r(\mu)) + (1 - \rho) \times [(1 - X(\mu))(T_u - T_0) + (X(\mu))(T_l - T_0)]] \times K_\lambda(T_0) B_\lambda(T_0).$$

The solution to this inversion problem is as follows.

*Step 1:* Since the leaves in both layers have the same spectral emissivity, we can calculate an intrinsic emissivity for  $T_0$  defined by the hemispheric averages of  $L_\lambda(\mu, T_0)$  and

$\epsilon_{\text{BRDF}}$ . Since for  $T_0$ ,  $\Delta\epsilon_{\text{GO}}$  must be zero, it is easy to show

$$B_\lambda(T_0) = \frac{E_\mu[L_\lambda]}{E_\mu[\epsilon_{\text{BRDF}}]} \quad (17)$$

where  $E_\mu[\ ]$  denotes the expectation (hemispheric average) of the quantity of interest. Using the ten simulated values described above and inverting  $B_\lambda$ , we obtain  $T_0 = 296.72$  K. If we reduce the number of data points to five (from  $\mu = 1.0$  to  $\mu = 2.0$  in steps of  $0.2$ ), the resulting  $T_0$  is  $296.79$  K. Therefore, we conclude that our estimate of  $T_0$  is stable. With  $T_0$  estimated from the average of all data, we now have three remaining unknowns.

*Step 2:* For every measurement  $L_\lambda(\mu, T_0)$  we have one equation

$$\begin{aligned} \frac{L_\lambda(\mu, T_0)}{B_\lambda(T_0)} - (1 - r(\mu)) \\ = (1 - \rho) \times [(1 - X(\mu))(T_u - T_0) + X(\mu)(T_l - T_0)] \\ \times K_\lambda(T_0). \end{aligned}$$

Reorganizing this equation, we get

$$D(\mu) = (T_u - T_0) + (T_l - T_u)X(\mu). \quad (18)$$

Using the five simulated observations, values for  $D(\mu)$  are listed in Table I.

Assuming that observations are available from multiple directions, we can use (18) to define a set of simultaneous equations. For example, if we have three angular measurements, then subtracting the first equation from the second and third, and then taking the ratio of the two, we obtain

$$\begin{aligned} (D(\mu_3) - D(\mu_1))(X(\mu_2) - X(\mu_1)) \\ = (D(\mu_2) - D(\mu_1))(X(\mu_3) - X(\mu_1)) \end{aligned}$$

where the subscripts refer to three distinct observations and fractional areas corresponding to  $D(\mu)$  and  $X(\mu)$ , respectively. Since  $X(\mu_i)$  is a known monotonic function of the unknown  $\Delta_{\text{LAI}}$  for each  $\mu$ , it is straightforward to solve this equation. For example, using  $\mu = 1.0, 0.8,$  and  $0.6$ , we get  $\Delta_{\text{LAI}} = 1.9986$ . If we use  $\mu = 0.6, 0.4,$  and  $0.2$ , we get

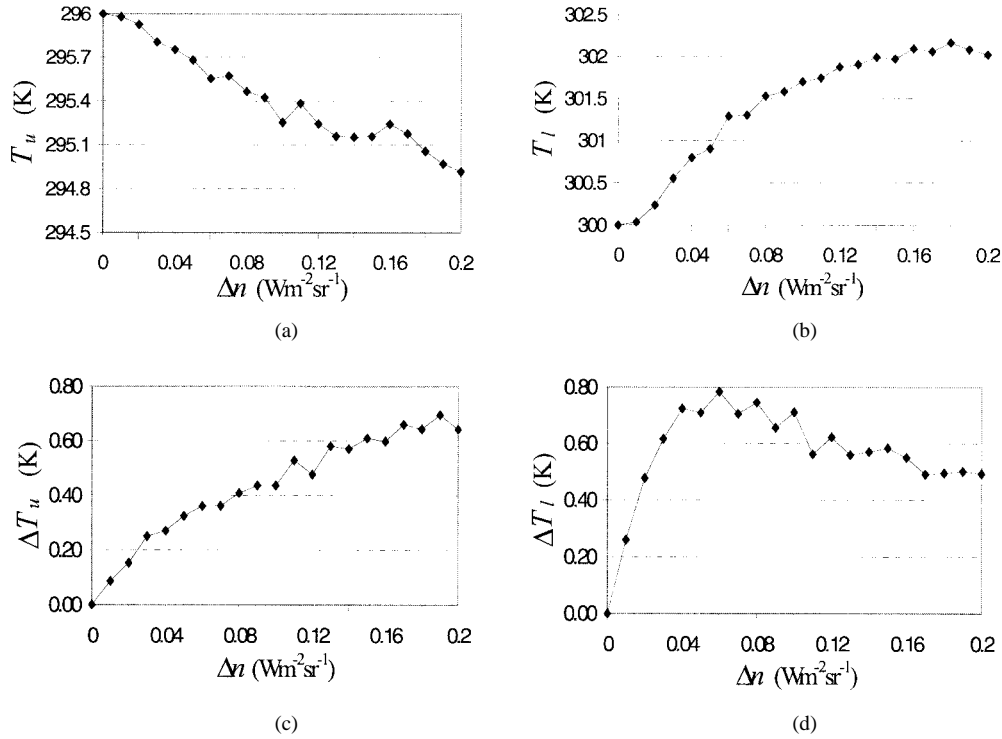


Fig. 4. Average results from inversions of  $T_u$  and  $T_l$  from 100 simulations in which Gaussian random noise was added to simulated directional radiances.

$\Delta_{LAI} = 2.0136$ . Once the value for  $\Delta_{LAI}$  is known, estimates for  $T_u$  and  $T_l$  can be obtained easily. For example, using  $\Delta_{LAI} = 1.9986$  for the two data points at  $\mu = 1.0$  and  $0.8$ , we have  $T_u = 295.97$  K and  $T_l = 299.92$  K, which are very close to the correct values of 296 and 300 K, respectively. Of course, the least squares method can be applied when more than three good measurements are available, but that is beyond the scope of this simple example.

Finally, we evaluated the sensitivity of model inversions to uncertainty in LST measurements. To do this, we performed 100 forward-mode simulations using the conceptual model to simulate LST values across eight view zenith angles ranging from 0 to  $80^\circ$ . Varying levels of Gaussian noise were added to the simulated radiance values, with standard deviations ranging from 0 to  $0.2 \text{ Wm}^{-2} \text{ sr}^{-1}$ . We then inverted the model using different combinations of view zenith angles. Representative results from this exercise are presented in Fig. 4 for inversions of  $T_l$  and  $T_u$ . These results show that some sensitivity to noise is clearly evident, especially for  $T_l$ .

## VI. CONCLUSIONS AND DISCUSSION

The purpose of this paper is to propose a conceptual model formally describing the directional emission of heterogeneous, nonisothermal surfaces. This model yields an effective LST that is independent of view angle and wavelength and an effective emissivity composed of two parts. The first part is a directional emissivity related to the emissivities of individual surface elements present within the sensor field of view. The second part is an apparent change in emissivity that arises from the temperature frequency distribution of individual surface elements.

Several inherent difficulties have precluded simultaneous and accurate definition of the average temperature and effective emissivity of nonisothermal surfaces using a single relation such as (6). One solution to this dilemma has been suggested by Dozier [11], and that is to identify the subpixel isothermal components. In the near future, when structural information becomes available from the moderate resolution imaging spectroradiometer (MODIS) BRDF product in association with accurate directional LST data from the MODIS LST product, we should be able to revisit the Dozier [11] idea for subpixel isothermal components instead of treating the surface as a nonisothermal mixture.

In order to do this, a physical model describing the directional thermal emission of such surfaces is required. Using a first-order Taylor series approximation, our model defines the effective emissivity of nonisothermal surfaces to consist of two parts: one intrinsic to the surface material and structure, the other caused by temperature differences among the surface components within the sensor field-of-view. This definition allows an average temperature to be defined independent of wavelength and viewing direction as required for use of the Planck function. If no application-specific definition of average temperature is required, our model also suggests a natural definition of average temperature that equates the hemispherical wide-band emissivity to the hemispherical re-emissivity. At the same time, the error caused by these approximations is minimized.

This new conceptual model explains the mechanism that gives rise to spectral and directional dependence in thermal emissions from nonisothermal surfaces by combining the merits of the DW BRDF model and the KSL GO model. It converges to the DW BRDF model when subpixel tem-

perature differences are small and converges to the KSL GO model when temperature differences are the dominant factor controlling the emission from nonisothermal surfaces.

Finally, it is important to note that this new model is instantaneous in nature. Process models to explain or predict changes of component temperatures are, of course, important. From a remote sensing perspective, however, it is necessary first to understand the relation between LST measurements and the directional emissivity of the surface at the moment when the satellite actually views it.

#### ACKNOWLEDGMENT

The authors have benefited from discussions with Dr. Z. Wan and Prof. R. Zhang as well as from Prof. R. Zhang's e-mail discussion with Prof. J. Norman and Prof. F. Becker. They also would like to thank G. Yan for generating the results presented in Fig. 4.

#### REFERENCES

- [1] L. Balick and B. Hutchinson, "Directional thermal infrared exitance distributions from a leafless deciduous forest," *IEEE Trans. Geosci. Remote Sensing*, vol. GE-24, pp. 693–698, Sept. 1986.
- [2] F. Becker, "The impact of spectral emissivity on the measurement of land surface temperature from a satellite," *Int. J. Remote Sensing*, vol. 8, no. 10, pp. 1509–1522, 1987.
- [3] F. Becker and Z.-L. Li, "Toward a local split window method over land surface," *Int. J. Remote Sensing*, vol. 11, no. 3, pp. 369–393, 1990.
- [4] ———, "Surface temperature and emissivity at various scales: Definition, measurement, and related problems," *Remote Sensing Rev.*, vol. 12, pp. 225–253, 1995.
- [5] P. J. Camillo, "Using one- or two-layer models for evaporation estimation with remotely sensed data," *Land Surface Evaporation: Measurements and Parameterization*, T. J. Schmugge and J. C. Andre, Eds. New York: Springer-Verlag, 1991.
- [6] T. N. Carlson, J. K. Dodd, S. G. Benjamin, and J. N. Cooper, "Satellite estimation of the surface energy balance, moisture availability and thermal inertia," *J. Appl. Meteorol.*, vol. 20, pp. 67–87, 1981.
- [7] T. N. Carlson, R. R. Gilles, and E. L. Perry, "A method to make use of thermal infrared temperature and NDVI measurements to infer surface soil water content and fractional vegetation cover," *Remote Sensing Rev.*, vol. 9, pp. 161–173, 1994.
- [8] V. Caselles and J. A. Sobrino, "Determination of frosts in orange groves from NOAA-9 AVHRR data," *Remote Sens. Environ.*, vol. 29, no. 2, pp. 135–146, 1989.
- [9] R. Crago, M. Sugita, and W. Brutsaert, "Satellite-derived surface temperatures with boundary layer temperatures and geostrophic winds to estimate surface energy fluxes," *J. Geophys. Res.*, vol. 100, no. D12, pp. 25 447–25 451, 1995.
- [10] G. R. Diak and M. S. Whipple, "Improvements to models and methods for evaluating the land-surface energy balance and effective roughness using radiosonde reports and satellite-measured skin temperature data," *Agric. Forest Meteorol.*, vol. 63, no. 3/4, pp. 189–218, 1993.
- [11] J. Dozier, "A method for satellite identification of surface temperature fields of subpixel resolution," *Remote Sensing Environ.*, vol. 11, pp. 221–229, 1981.
- [12] J. Dozier and S. G. Warren, "Effect of viewing angle on the infrared brightness temperature of snow," *Water Resources Res.*, vol. 18, no. 5, pp. 1424–1434, 1982.
- [13] M. A. Friedl, "Modeling land surface fluxes using a sparse canopy model and radiometric temperature measurements," *J. Geophys. Res.*, vol. 100, no. D12, pp. 25 435–25 446, 1985.
- [14] A. R. Gillespie, R. Rokugawa, S. J. Hook, T. Matsunaga, and A. B. Kahle, "Temperature/emissivity separation algorithm theoretical basis document," Version 2.3, Available: <http://asterweb.jpl.nasa.gov/asterhome/atbd/docs.htm>, p. 74, 1996.
- [15] B. W. Hapke, "Bidirectional reflectance spectroscopy 1: Theory," *J. Geophys. Res.*, vol. 86, no. B4, pp. 3039–3054, 1981.
- [16] R. D. Jackson, R. J. Reginato, and S. B. Idso, "Wheat canopy temperature: A practical tool for evaluating water requirements," *Water Resources Res.*, vol. 13, no. 3, pp. 651–656, 1977.
- [17] A. Kahle, "A simple thermal model of the Earth's surface for geological mapping by remote sensing," *J. Geophys. Res.*, vol. 82, pp. 1673–1680, 1977.
- [18] A. B. Kahle, D. P. Madura, and J. M. Soha, "Middle infrared multispectral aircraft scanner data: Analysis for geological applications," *Appl. Opt.*, vol. 19, pp. 2279–2290, 1980.
- [19] H. Kerdiles, M. Grondana, R. Rodriguez, and B. Seguin, "Frost mapping using NOAA AVHRR data in the Pampean region, Argentina," *Agric. Forest Meteorol.*, vol. 79, no. 3, pp. 157–182, 1996.
- [20] D. S. Kimes, J. A. Smith, and L. E. Link, "Thermal IR exitance model of a plant canopy," *Appl. Opt.*, vol. 20, no. 4, pp. 623–632, 1981.
- [21] F. Kimura and A. P. Shimizu, "Estimation of sensible and latent heat fluxes from soil surface temperature using a linear air land heat transfer model," *J. Appl. Meteorol.*, vol. 33, no. 4, pp. 477–489, 1994.
- [22] W. P. Kustas, R. Jackson, and G. Asrar, "Estimating surface energy balance components from remotely sensed data," in *Theory Applications of Optical Remote Sensing*. New York: Wiley, 1989, pp. 604–627.
- [23] X. Li and A. Strahler, "Geometric-optical bidirectional reflectance modeling of a coniferous forest canopy," *IEEE Trans. Geosci. Remote Sensing*, vol. GE-24, pp. 281–293, Nov. 1986.
- [24] X. Li, A. Strahler, and C. Woodcock, "A hybrid geometric optical-radiative transfer approach for modeling albedo and directional reflectance of discontinuous canopies," *IEEE Trans. Geosci. Remote Sensing*, vol. 33, pp. 466–480, Mar. 1995.
- [25] Z.-L. Li and F. Becker, "Feasibility of land surface temperature and emissivity determination from AVHRR data," *Remote Sens. Environ.*, vol. 43, pp. 67–85, 1993.
- [26] Q. Liu, X. Xu, and J. Chen, "An iterative inversion for remote sensing of LST/emissivity—I: Theory and simulation," *J. Remote Sensing*, vol. 2, no. 1, pp. 1–8, 1998 (in Chinese).
- [27] J. Norman and F. Becker, "Terminology in thermal infrared remote sensing of natural surfaces," *Agric. Forest Meteorol.*, vol. 77, no. 3–4, pp. 153–176, 1995.
- [28] A. J. Prata, "Land surface temperatures derived from the advanced very high resolution radiometer and the along-track scanning radiometer—2: Experimental results and validation of AVHRR algorithms," *J. Geophys. Res.*, vol. 99, no. D6, pp. 13 025–13 058, 1994.
- [29] J. C. Price, "The potential of remotely sensed thermal infrared data to infer surface soil moisture and evaporation," *Water Resources Res.*, vol. 1, no. 4, pp. 787–795, 1980.
- [30] ———, "Estimating surface temperature from satellite thermal infrared data—A simple formulation for the atmospheric effect," *Remote Sens. Environ.*, vol. 13, pp. 353–361, 1983.
- [31] ———, "Land surface temperature measurements from the split window channels of the NOAA-7 AVHRR," *J. Geophys. Res.*, vol. 79, pp. 5039–5044, 1984.
- [32] ———, "Quantitative aspects of remote sensing in the thermal infrared," in *Theory and Applications of Optical Remote Sensing*, G. Asrar Ed. New York: Wiley, 1989, ch. 15, pp. 578–603.
- [33] V. J. Realmuto, "Separating the effects of temperature and emissivity: Emissivity spectrum normalization," in *Proc. 2nd TIMS Workshop*, JPL-Pub. 90-55, 1990, pp. 31–35.
- [34] T. J. Schmugge and F. Becker, "Remote sensing observations for the monitoring of land-surface fluxes and water budgets," in *Land Surface Evaporation: Measurements and Parameterization*, T. J. Schmugge and J. C. Andre, Eds. New York: Springer-Verlag, 1991.
- [35] W. Snyder and Z. Wan, "BRDF models to predict spectral reflectance and emissivity in the thermal infrared," *IEEE Trans. Geosci. Remote Sensing*, vol. 36, pp. 214–225, Jan. 1998.
- [36] H. Tonooka and T. Hoshi, "Feasibility of atmospheric and surface parameters determination from TIR multispectral data over land," in *Proc. 17th Asian Conf. Remote Sensing*, G7, 1996, pp. 1–6.
- [37] R. C. Vining and B. L. Blad, "Estimation of sensible heat flux from remotely sensed canopy temperatures," *J. Geophys. Res.*, vol. 97, no. D17, pp. 18 951–18 954, 1992.
- [38] Z. Wan and J. Dozier, "A generalized split-window algorithm for retrieving land-surface temperature from space," *IEEE Trans. Geosci. Remote Sensing*, vol. 34, pp. 892–905, July 1996.
- [39] ———, "Land-surface temperature measurement from space: Physical principles and inverse modeling," *IEEE Trans. Geosci. Remote Sensing*, vol. 27, no. 3, pp. 268–278, 1989.
- [40] Z. Wan and Z.-L. Li, "A physics-based algorithm for retrieving land-surface emissivity and temperature from EOS/MODIS data," *IEEE Trans. Geosci. Remote Sensing*, vol. 35, pp. 980–996, July 1997.
- [41] K. Watson, "Geological application of TIR images," *Proc. IEEE*, vol. 63, no. 1, pp. 128–137, 1975.
- [42] L. Zhang, R. Lemeur, and J. P. Goutorbe, "A one-layer resistance model for estimating regional evapotranspiration using remote sensing data," *Agric. Forest Meteorol.*, vol. 77, no. 3–4, pp. 241–261, 1995.

**Xiaowen Li** graduated from the Chengdu Institute of Radio Engineering, China, in 1968. He received the M.A. degree in geography and the M.S. degree in electrical and computer engineering and the Ph.D. degree in geography from the University of California, Santa Barbara, in 1981 and 1985, respectively.

He is currently with the Research Center for Remote Sensing and GIS, Beijing Normal University, China. Before this, he was a Professor at the Institute of Remote Sensing Applications of the Chinese Academy of Science, Beijing, while simultaneously holding the position of Research Professor at the Center for Remote Sensing, Department of Geography, Boston University, Boston, MA. His primary research interests are in 3-D modeling of reflectance and thermal emission of land surfaces (vegetation in particular) and information extraction from mutiangular, remotely sensed images.

**Alan H. Strahler** (M'86), for a photograph and biography, see p. 738 of the March 1999 issue of this TRANSACTIONS.

**Mark A. Friedl**, for a biography, see p. 977 of the March 1999 issue of this TRANSACTIONS.